Variation of the Jahn–Teller distortion with pressure in the layered perovskite Rb_2CuCl_4: local and crystal compressibilities

2007 J. Phys.: Condens. Matter 19 346229

(http://iopscience.iop.org/0953-8984/19/34/346229)

IOP PUBLISHING JOURNAL OF PHYSICS: CONDENSED MATTER

J. Phys.: Condens. Matter **19** (2007) 346229 (9pp) doi:10.1088/0953-8984/19/34/346229

Variation of the Jahn–Teller distortion with pressure in the layered perovskite Rb_2CuCl_4: local and crystal compressibilities

F Aguado[1], F Rodríguez[1,5], R Valiente[2], M Hanfland[3] and J P Itié[4]

[1] DCITIMAC, Facultad de Ciencias, Universidad de Cantabria, Santander 39005, Spain
[2] Departamento de Física Aplicada, Universidad de Cantabria, Santander 39005, Spain
[3] ESRF, BP220, 156 rue des Martires, 38043 Grenoble Cedex, France
[4] Université Pierre et Marie Curie, B77 4 Place Jussieu 75252 Paris Cedex 05, France

E-mail: rodriguf@unican.es

Received 2 May 2007, in final form 26 June 2007
Published 31 July 2007
Online at stacks.iop.org/JPhysCM/19/346229

Abstract

This work investigates the effect of pressure on the Jahn–Teller distortion (JTD) associated with the axially elongated $CuCl_6$ octahedra in the A_2CuCl_4 perovskite layer (A: Rb, CH_3NH_3, $C_2H_5NH_3$, $C_3H_7NH_3$). The aim is to elucidate whether pressure favours disappearance of the JTD in the antiferrodistortive (AFD) structure exhibited by Cu^{2+} within the layers or whether it induces tilts of the $CuCl_6$ octahedra preserving the molecular distortion associated with the JT effect. We have carried out x-ray absorption (XAS) and x-ray diffraction (XRD) experiments under pressure along the compound series, whose interlayer distances at ambient pressure vary from 7.77 to 12.33 Å. The use of both XAS and XRD techniques allows us a complete local- and crystal-structure characterization in Rb_2CuCl_4 as a function of pressure in the 0–16 GPa range. We show that pressure reduces the axial (long) and equatorial (short) Cu–Cl distances, R_{ax} and R_{eq}, as well as the intralayer and interlayer Cu–Cu distances, d_{Cu-Cu} and d_{inter}. Interestingly, the variation of R_{ax} is an order of magnitude bigger than that of the corresponding R_{eq}, yielding a reduction of the JTD. However, no evidence of JTD suppression has been observed below 16 GPa. Pressure-induced $CuCl_6$ tilting preserves the JTD in a wide pressure range. Estimates based on structural data suggest that JT suppression would occur at about 40 GPa.

(Some figures in this article are in colour only in the electronic version)

[5] Author to whom any correspondence should be addressed.

1. Introduction

A_2CuCl_4 (A = Rb, $C_nH_{2n+1}NH_3$) layered perovskites involve an ample variety of interesting physical phenomena related to the Jahn–Teller (JT) Cu^{2+} ions ($3d^9$ configuration), and their magnetic coupling within the layer [1–4]. The axially elongated $CuCl_6$ octahedra display an intralayer antiferrodistortive (AFD) structure (figure 1), which is characterized by the alternation of $d_{x^2-y^2}$ and $d_{y^2-z^2}$ orbitals in the plane favouring ferromagnetic interaction between intralayer Cu–Cu ions. Unlike Mn^{3+} isomorphous $AMnF_4$, whose JT MnF_6 units exhibit a significant tilting (Mn–F–Mn $< 162°$), the Cu–Cl–Cu bond angle in halide perovskites is close to 180° (nearly ideal perovskite), making it responsible for the intralayer ferromagnetic exchange interaction [5]. By contrast, the interlayer exchange interaction is about three or four orders of magnitude weaker, and can be ferromagnetic or antiferromagnetic depending on the relative Cu–Cu interlayer distance and the tilting of $CuCl_6$ octahedra [4]. Interestingly, the interplay between JT distortion (JTD) and tilting, and its effect on the physical properties of layered perovskites have motivated our research to establish structural correlations. An intense activity has been focussed on both Cu^{2+}- and Mn^{3+}-related compounds to find out structural requirements to get either insulating ferromagnets [3, 4, 6] or pressure-induced disappearance of the AFD structure [7–12]. In perovskite halides involving Cu^{2+}, no indication of bulk ferromagnetism beyond $(CH_3NH_3)_2CuCl_4$ and K_2CuF_4 has been found. Furthermore no clear evidence of pressure-induced JT suppression has been reported for these compounds. Nevertheless, the application of either chemical or hydrostatic pressure changes the magnetic behaviour of these compounds. Whereas a change of the three-dimensional (3D) magnetism from antiferromagnetism to ferromagnetism is attained on passing from $n = 2$ or 3 to 1 in $(C_nH_{2n+1}NH_3)_2CuCl_4$ (increase of chemical pressure), hydrostatic pressure induces a switch from ferromagnetism to antiferromagnetism in $(CH_3NH_3)_2CuCl_4$ [10] and K_2CuF_4 [13–16]. However, Rb_2CuCl_4 is antiferromagnetic ($T_N = 13.8$ K) although it presents the shortest interlayer distance in the A_2CuCl_4 series [4]. In addition this compound is interesting since it provides an in-layer Cu–Cl–Cu angle of 180° at ambient conditions (ideal perovskite).

It is worth pointing out that the structural variation undergone by this compound family under pressure still remains unclear in spite of the intense research carried out on the magnetic and optical properties as a function of pressure [3, 4, 17, 18]. Correlation studies between lattice parameters from XRD and Cu–Cl bond distances from the extended x-ray absorption fine structure (EXAFS) in $(C_3H_7NH_3)_2CuCl_4$ [19] showed that although the reduction of the Cu–Cl axial distance with pressure, ΔR_{ax}, is longer than ΔR_{eq}, in no way is the JTD suppressed below 10 GPa. However, recent XRD experiments in the isomorphous $(C_2H_5NH_3)_2CuCl_4$ reports that JT suppression takes place along with a structural phase transition at 4 GPa [12]. A similar situation occurred for $LaMnO_3$ [20, 21]. Neutron diffraction under pressure indicates that the MnO_6 JTD is stable in the 0–6 GPa range [20], whereas XRD reveals that pressure gradually reduces the JTD, yielding suppression at about 10 GPa [21]. This controversy is likely due to difficulties to perform a precise analysis of the diffracted intensities, providing the M–X bond distances of the MX_6 polyhedron. In general, the M–X distances and their variation with pressure in perovskites can be difficult in cases where the structural information cannot be derived from the cell parameters but through intensity analysis. The problem is even harder if, as in the present case, we deal with AFD structures. XRD powder diagrams often exhibit intensity deviations due to preferential orientation, twining, texture and dynamical JT effects that can hinder analysis of the diffracted intensity associated with JTD. The use of local probes like EXAFS or optical absorption (OA) spectroscopy can be crucial to cope with structural determination [6, 19]. However, it must be pointed out that suitable powder XRD patterns can be obtained for intensity analysis in pressure experiments provided that we

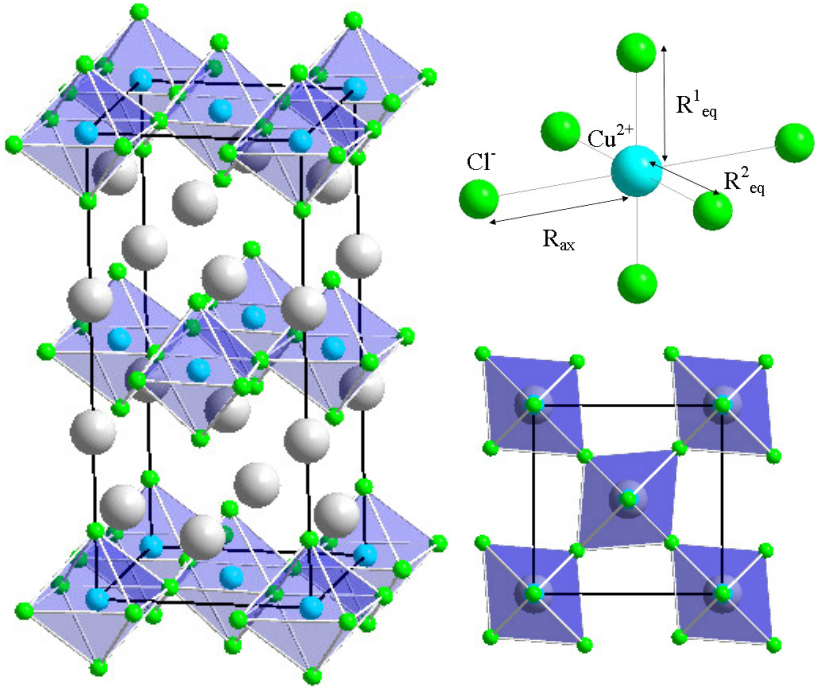

Figure 1. (Left) Crystal structure of the Rb_2CuCl_4-layered perovskite at ambient conditions; orthorhombic *Acam*: $a = 7.187(4)$ Å, $b = 7.197(4)$ Å and $c = 15.534(6)$ Å. (Right) View of the $CuCl_6$ nearly tetragonal octahedra with the three different Cu–Cl distances: $R_{ax} = 2.72$ Å and $R_{eq} = 2.35$ Å (top). View of the *a*–*b* plane (bottom). Note the antiferrodistortive structure displayed by the $CuCl_6$ units.

fulfil the strict sample requirements imposed by the diamond anvil cell (DAC). Failures due to sample handling, texture and detection system are usual causes for erroneous reported data from pressure experiments.

In this work we investigate the effects of pressure on the crystal and local structure around Cu^{2+} in Rb_2CuCl_4. In particular, we focus on how pressure modifies the JTD associated with the axially elongated $CuCl_6$ octahedra and compare it with previous results on $(C_3H_7NH_3)_2CuCl_4$ [19] and $(C_2H_5NH_3)_2CuCl_4$ [12]. The aim is to elucidate whether pressure can suppress the JTD exhibited by Cu^{2+}, and therefore the AFD structure of the layer, or induce tilts of the $CuCl_6$ octahedra, but preserving the molecular distortion associated with the JT effect. For this purpose, we have carried out x-ray absorption (XAS) and x-ray diffraction (XRD) experiments under pressure. The use of both XAS and XRD techniques allows us a complete structural characterization, which is difficult to accomplish from powder XRD in Rb_2CuCl_4.

2. Experimental details

Single crystals of Rb_2CuCl_4 (1–0.1 mm^3) were grown from dried methyl alcohol solutions. A saturated solution of RbCl in methanol was poured into $CuCl_2$ methanol solution, using appropriate stoichiometric amounts of RbCl and $CuCl_2$. After several minutes red-brownish single crystals precipitate. The orthorhombic *Acam* space group was checked by

Table 1. Structural parameters for A_2CuCl_4 (A = Rb, $C_nH_{2n+1}NH_3$; $n = 1$–3) layered perovskites at ambient conditions. d_{inter} and d_{Cu-Cu} are the interlayer distance and the intralayer Cu–Cu distance ($d_{Cu-Cu} = 1/2(a^2 + b^2)$), respectively. R_{ax} and R_{eq} are the axial and equatorial Cu–Cl distances, where $R_{eq} = \frac{1}{2}(R_{1eq} + R_{2eq})$ (see figure 1). The normal coordinates are $Q_\theta = \frac{2}{\sqrt{3}}(R_{ax} - R_{eq})$ and $Q_\varepsilon = R_{2eq} - R_{1eq}$.

	Crystal structure							Local structure				
Compound	Space group	a (Å)	b (Å)	c (Å)	V (Å^3)	d_{Cu-Cu} (Å)	d_{inter} (Å)	R_{ax} (Å)	R_{eq} (Å)	Q_θ (Å)	Q_ε (Å)	Ref.
$(C_3H_7NH_3)_2CuCl_4$	*Pbca*	7.65	7.33	24.66	1382.8	5.30	12.33	3.04	2.29	0.87	0.002	[27]
$(C_2H_5NH_3)_2CuCl_4$	*Pbca*	7.47	7.35	21.18	1162.9	5.24	10.59	2.98	2.28	0.80	0.008	[26]
$(CH_3NH_3)_2CuCl_4$	$B2_1/a$	7.370	7.269	18.648	999.0	5.18	9.33	2.91	2.28	0.71	0.014	[25]
Rb_2CuCl_4	*Acam*	7.187	7.197	15.534	803.5	5.09	7.77	2.72	2.35	0.43	0.046	[22]

x-ray diffraction. The room-temperature parameters obtained are the same as those given elsewhere [22]: $a = 7.187(4)$ Å, $b = 7.197(4)$ Å and $c = 15.534(6)$ Å (figure 1). All compounds were handled in a globe box under argon atmosphere in order to avoid hydration. In contact with air, the crystal transforms into the hydrate $Rb_2CuCl_4(H_2O)_2$ phase [23], which is tetragonal ($P4_2/mnm$ space group) with lattice parameters $a = b = 7.596$ Å, and $c = 8.027$ Å. Partial or total hydration can be easily identified by powder XRD and its characteristic yellow-greenish colour.

XRD under pressure was performed in the ID9 white beam station at the ESRF in Grenoble. Experiments were done on a diamond anvil cell (DAC) at room temperature using helium as the pressure transmitter. X-ray powder diffractograms were obtained using an image-plate detector as a function of pressure in the 0–15 GPa range with $\lambda = 0.4131$ Å, which is far enough from the spectral region of the diamond absorption. XAS under pressure was performed at the absorption setup XAS10 of the D11 beamline at LURE (Orsay). Pressure was applied with a membrane-type DAC using silicon oil as the pressure transmitter. EXAFS spectra of the investigated Rb_2CuCl_4 were measured at the Cu K edge ($E_0 = 8.98$ keV) at room temperature using dispersive XAS in the 8.9–9.3 keV range. This experimental set-up has been proved to be very sensitive for obtaining suitable EXAFS oscillations in a wavelength range where the diamond anvil absorption is very strong. In both cases pressure was measured from the R-line shift of ruby. The XRD and XAS data were analysed by means of the FullProf [24] and the WINXAS package programs, respectively.

3. Results and discussion

The structural parameters at ambient conditions for Rb_2CuCl_4 are shown in table 1 together with the corresponding data of A_2CuCl_4 (A = $C_nH_{2n+1}NH_3$; $n = 1$–3). Note that the interlayer distance ($d_{inter} = c/2$) decreases with the size of the A cation from 12.33 Å in $(C_3H_7NH_3)_2CuCl_4$ to 7.77 Å in Rb_2CuCl_4. Moreover, the interlayer decrease along the series is accompanied by a reduction of the local $CuCl_6$ volume, which correlates with a partial reduction of the JTD. The octahedral normal coordinate, $Q_\theta = 2/\sqrt{3}\,(R_{ax} - R_{eq})$, shows that the JTD, Q_θ, decreases from 0.87 Å in $(C_3H_7NH_3)_2CuCl_4$ to 0.43 Å in Rb_2CuCl_4. However, the Cu–Cl–Cu bond angle varies from 166.6° to 180°, thus evolving to an ideal perovskite with the crystal-volume reduction. From the cation substitution along the series (chemical-pressure effect), we can draw two main conclusions: (i) crystal contraction reduces the $CuCl_6$ JTD; (ii) the Cu–Cl–Cu bond angle tends to the ideal perovskite value (180°). It must be noted

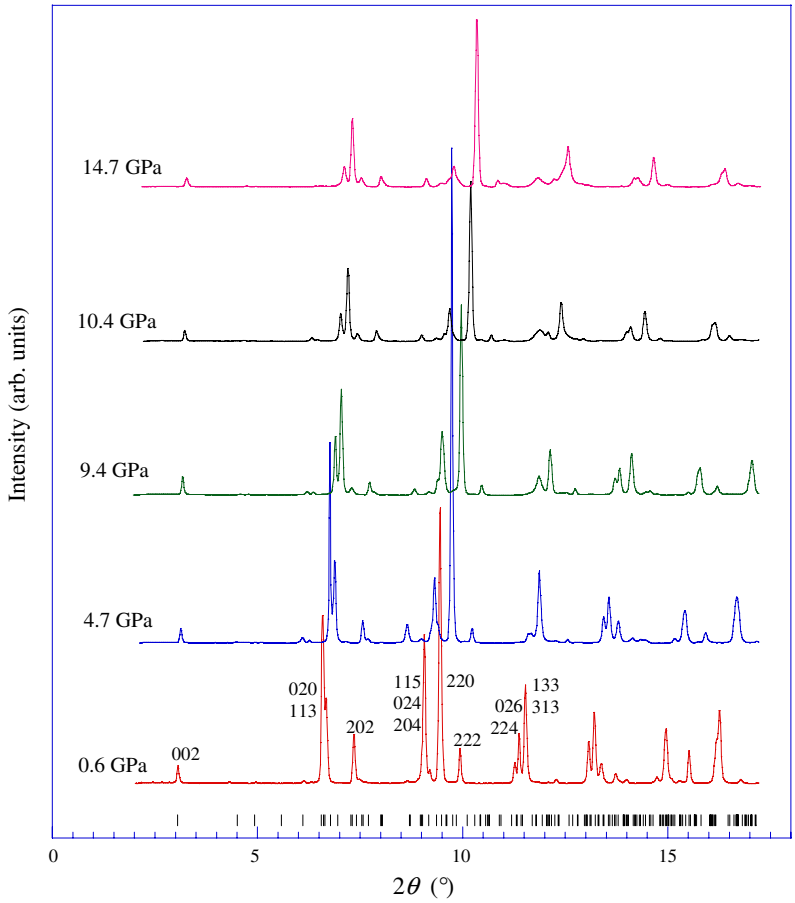

Figure 2. Variation of XRD pattern of Rb_2CuCl_4 as a function of pressure. The vertical bars indicate the calculated Bragg reflections of the compound in the *Pbca* space group at ambient pressure. The Miller indices corresponding to the more intense peaks are included.

that the chemical-pressure effect is very anisotropic since the relative intralayer contraction is an order of magnitude smaller than the interlayer contraction, due to the size of the substituted cation. The question arising is whether hydrostatic pressure induces analogous structural effects on Rb_2CuCl_4.

Figure 2 shows the XRD evolution of Rb_2CuCl_4 with pressure. XRD patterns in the whole 0–16 GPa pressure range can be indexed on the basis of the same ambient-pressure *Acam* orthorhombic structure, although we used a general *Pbca* orthorhombic space group in order to allow for structural distortions associated with octahedra tilts. The XRD analysis shows no indication of structural transitions to a monoclinic structure. The absence of splitting in the (113), (220) and (222) Bragg peaks supports this view. The variation of the lattice parameters and the cell volume with the corresponding Murnaghan equation-of-state (EOS) parameters are shown in figure 3. We observe an anomaly in the volume variation, $V(P)$, at about 3 GPa associated to a pressure-induced phase transition likely related to another orthorhombic high-pressure phase. Interestingly, the obtained bulk moduli, $B_0 = 19.7$ and 23.6 GPa in the low- and high-pressure phases, respectively, are bigger than those measured

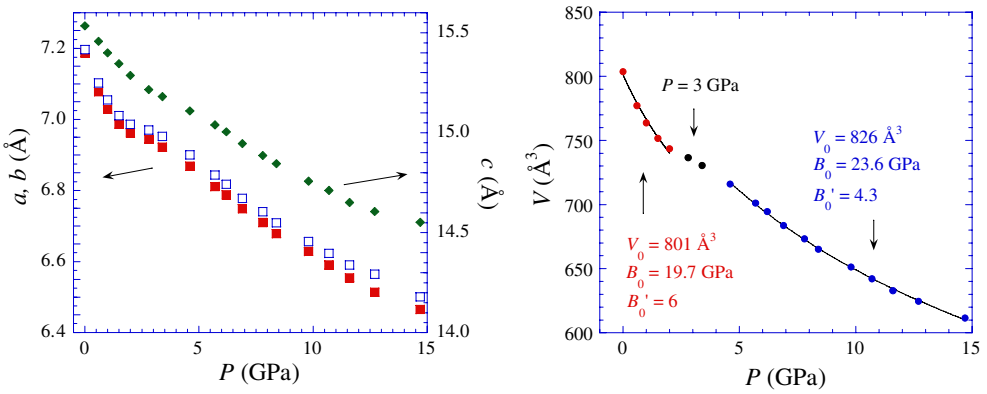

Figure 3. (Left) Variation of the lattice parameters of Rb_2CuCl_4 with pressure. Note the different behaviour around 3 GPa, suggesting that a structural phase transition takes place in such a pressure range. (Right) Crystal cell-volume variation as a function of pressure. The solid lines correspond to the least-square fittings to the Murnaghan equation of state with the parameters displayed in the figure for both structural phases.

for $(C_3H_7NH_3)_2CuCl_4$, $B_0 = 7.1$ GPa [19], and $(C_2H_5NH_3)_2CuCl_4$, $B_0 = 8.4$ GPa [12], but three times smaller than the local bulk modulus measured for $CuCl_6$, $B_{loc} = 63$ GPa, in $(C_3H_7NH_3)_2CuCl_4$ [19]. This result clearly suggests that pressure induces octahedron tilting in Rb_2CuCl_4 provided that the local bulk modulus for $CuCl_6$ has a similar value. Furthermore the intralayer Cu–Cu distance, d_{Cu-Cu}, varies from 5.09 to 4.58 Å from ambient pressure to 15 GPa (figure 3). The variation, $\Delta d_{Cu-Cu} = -0.51$ Å, would lead to a reduction of the axial distance, $\Delta R_{ax} \approx -0.45$ Å, provided that $\Delta R_{eq} \approx -0.05$ Å, and the ideal perovskite structure (Cu–Cl–Cu angle, $\phi = 180°$) remains under pressure, thus yielding suppression of the JT effect. Given that the local structure of $CuCl_6$ changes slightly in the explored pressure range we conclude that $CuCl_6$ octahedra experience tilting phenomena under pressure. This tilting scenario makes the bulk-volume reduction compatible with the stability of the JTD.

Figure 4 shows the variation of XAS around the Cu K edge in Rb_2CuCl_4 as a function of pressure. The analysis of the EXAFS region provides the structural parameters given in figure 5 (left). EXAFS spectra were fitted on the basis of a $CuCl_6$ structural unit of D_{4h} symmetry due to the reduced number of oscillations available using DACs. With this structural model we were able to obtain reliable Cu–Cl bond length variations from the XAS spectra of figure 4. The linear dependence of R_{eq} and R_{ax} with pressure is shown in figure 5 together with the variations experienced by the intralayer Cu–Cu distance derived from XRD as $d_{Cu-Cu} = 1/2\,(a^2 + b^2)^{1/2}$ with $d = R_{ax} + R_{eq}$, derived from EXAFS. The two distances d_{Cu-Cu} and d should coincide if $\phi = 180°$ in the whole pressure range. Actually, the comparison of d_{Cu-Cu} and d provides direct evidence on the tilting phenomena in Rb_2CuCl_4. In particular, we would expect an evolution of the Cu–Cl–Cu angle towards 180° if the pressure variation Δd_{Cu-Cu} is shorter than $\Delta(R_{ax} + R_{eq})$, while the opposite would occur if $\Delta d_{Cu-Cu} > \Delta(R_{ax} + R_{eq})$. Therefore XAS and XRD results clearly show that pressure induces $CuCl_6$ tilts in Rb_2CuCl_4 rather than JTD suppression. Indeed, we do observe a progressive reduction of R_{ax} and R_{eq} with pressure, i.e. the JTD. The axial distance variation in the 0–15 GPa range, $\Delta R_{ax} = -0.18$ Å, is an order of magnitude bigger than $\Delta R_{eq} = -0.01$ Å. This means that, besides tilting, pressure also induces a progressive reduction of the JTD, which is $\Delta Q_\theta = -0.2$ Å from 0.6 to 15.9 GPa (figure 5 (left)). According to present data, the JTD at 15 GPa is reduced to almost one half its ambient pressure value. Simple linear extrapolation of R_{ax} and R_{eq} indicates that the JT

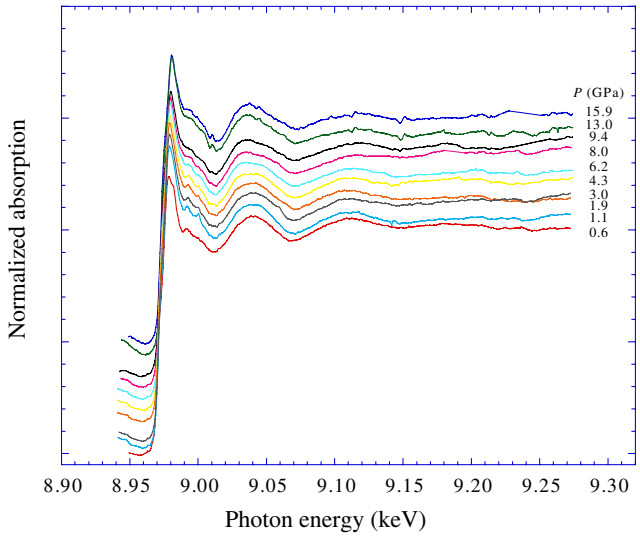

Figure 4. Variation of XAS for Rb_2CuCl_4 as a function of pressure. No evidence of drastic changes of local structure around Cu^{2+} is found from the XANES variation with pressure.

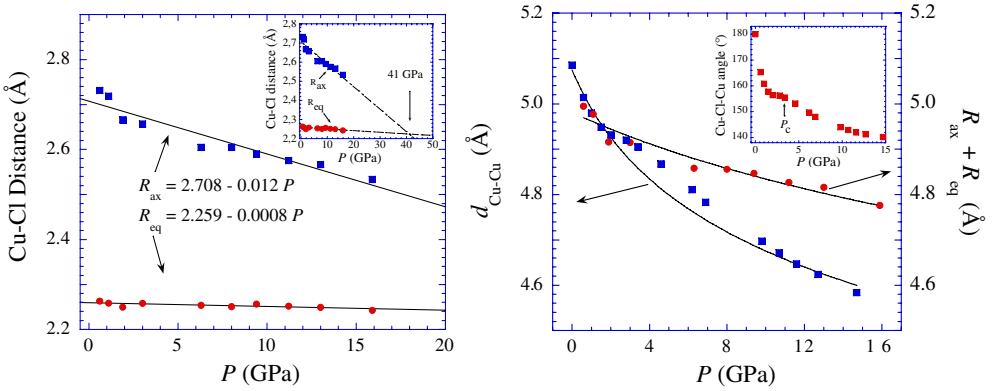

Figure 5. (Left) Variation of the local Cu–Cl bond distances (R_{ax} and R_{eq}) in Rb_2CuCl_4 with pressure. The inset shows the extrapolation of data up to 50 GPa. Note that disappearance of the JTD in $CuCl_6$ is expected at 41 GPa. (Right) Variation of intralayer Cu–Cu distance (d_{Cu-Cu}) derived from XRD and the sum, $d = R_{ax} + R_{eq}$, derived from XAS. The inset shows the Cu–Cl–Cu tilting angle calculated from $\varphi = \arccos\left(\frac{d^2_{Cu-Cu} - R^2_{ax} - R^2_{eq}}{-2R_{ax}R_{eq}}\right)$. Note that d_{Cu-Cu} is different from $R_{ax} + R_{eq}$ at ambient pressure due to EXAFS uncertainties.

suppression would occur about 41 GPa (see the inset to figure 5 (left)). A similar pressure value was also estimated for $(C_3H_7NH_3)_2CuCl_4$ [19]. However, it is worth pointing out that the present results really differ from the reported values (4 GPa) derived from Raman [7] and XRD [12] experiments in the isomorphous $(C_2H_5NH_3)_2CuCl_4$. In view of the present structural study we conclude that the use of the Raman technique for this purpose is subtle since peak disappearance may be somehow related to tilting dynamics rather than transformations of $CuCl_6$ local structure yielding JTD suppression.

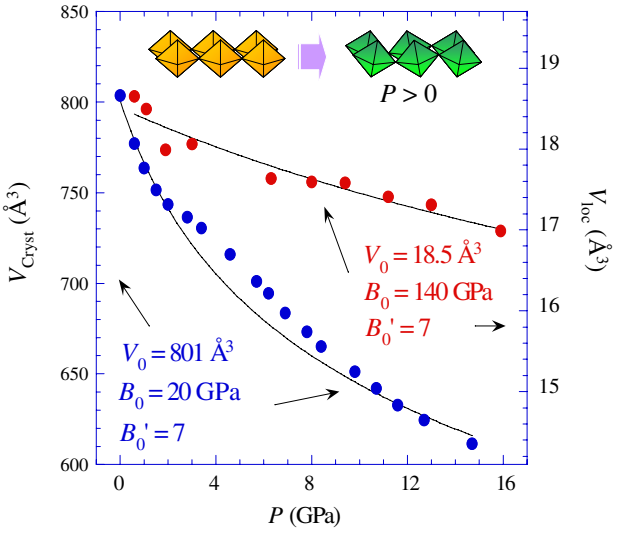

Figure 6. Pressure dependence of the local $CuCl_6$ volume, $V_{loc} = 4/3 \cdot R_{ax} \cdot R_{eq}^2$, and the orthorhombic cell volume, $V_{Cryst} = a \cdot b \cdot c$, in Rb_2CuCl_4 with pressure. The curves represent least-square fits to a Murnaghan EOS using the same equation in the whole pressure range but excluding data points around the transition pressure at 3 GPa. The obtained fitting parameters (zero-pressure volume, V_0; bulk modulus, B_0) and the corresponding pressure derivative, B_0', are nearby included.

Anyhow, the high-pressure range required to suppress the JTD, 41 GPa, in Rb_2CuCl_4 (figure 5), could be anticipated from the JT energy of $CuCl_6$ derived from optical absorption spectroscopy, $E_{JT} = 0.3$ eV/Cu [3]. This JT energy and the associated distortion, $Q_\theta = 0.43$ Å, likely suggest that the JT suppression pressure at which $Q_\theta = 0$ must be above 20 GPa, confirming the present estimates. Figure 6 compares the variations of the crystal and local volumes with pressure. The fit to a Murnaghan EOS provides a local bulk modulus for $CuCl_6$, $B_0 = 140$ GPa, whereas the mean crystal bulk modulus $B_0 = 20$ GPa, indicating that the crystal is seven times more compressible than $CuCl_6$ octahedra, thus confirming the proposed pressure structural variation based on tilts. Furthermore, the local EOS indicates that the pressure required to release the JT energy ($E_{JT} = 0.3$ eV/Cu) for JTD suppression is 35 GPa, in fair agreement with extrapolated data.

4. Conclusions

From XRD and EXAFS of Rb_2CuCl_4 we conclude that pressure induces reduction of the Cu–Cl distances, R_{ax} and R_{eq}, of the axially elongated $CuCl_6$ octahedron as well as the intralayer and interlayer Cu–Cu distances. Interestingly, the pressure-induced $CuCl_6$ tilting phenomenon is associated with the different compressibility of the bulk crystal and the $CuCl_6$ octahedron. Besides the anisotropic contraction of the crystal, the $CuCl_6$ compressibility is seven times smaller than the crystal compressibility. This large difference has been related to the stiffness of the Cu–Cl bonds associated with the JT effect, which preserves the $CuCl_6$ JTD in a wide range of pressure up to 20 GPa, according to experimental data and estimates based on the JT energy ($E_{JT} = 0.3$ eV/Cu). As a salient conclusion we show that in these layered perovskites pressure induces both octahedron tilts and JTD reduction, although no indication of JT suppression is found in the 0–16 GPa range. The present results can clarify the controversial pressure behaviour described in other Jahn–Teller systems, e.g. Mn^{3+} in oxides.

Acknowledgments

We thank Dr Julio Pellicer for fruitful discussions on XAS data. This work was financed by the Spanish MEyC (Project Ref. MAT2005-00099). FR acknowledges partial support from the I3 Research Intensification Program of the University and the Autonomous Government of Cantabria. The XAS and XRD experiments were done under a proposal at D11/LURE (Project PS 048-03), and ID09A/ESRF (Project HS2159), respectively.

References

[1] Reinen D and Atanasov M 1991 *Magn. Reson. Rev.* **15** 167
[2] Hitchman M A 1994 *Comment Inorg. Chem.* **15** 197
[3] Valiente R and Rodríguez F 1999 *Phys. Rev.* B **60** 9423
[4] Aguado F, Rodríguez F, Valiente R and Señas A 2004 *J. Phys.: Condens. Matter* **16** 1927
[5] Khomskii D I and Kugel K I 1973 *Solid State Commun.* **13** 763
[6] Rodríguez F and Aguado F 2003 *J. Chem. Phys.* **118** 10867
[7] Moritomo Y and Tokura Y 1994 *J. Chem. Phys.* **101** 1763
[8] Narita N and Yamada I 1996 *J. Phys. Soc. Japan* **65** 4054
[9] Manaka H, Yamada I, Nishi M and Goto T 2001 *J. Phys. Soc. Japan* **70** 241
[10] Manaka H, Yamada I, Nishi M and Goto T 2001 *J. Phys. Soc. Japan* **70** 1390
[11] Manaka H, Yamada I and Goto T 2002 *J. Phys. Soc. Japan* **71** 2822
[12] Ohwada K, Ishii K, Inami T, Murakami Y, Shobu T, Ohsumi H, Ikeda N and Ohishi Y 2005 *Phys. Rev.* B **72** 014123
[13] Ishizuka M, Terai M, Hidaka M, Endo S, Yamada I and Shimomura O 1998 *Phys. Rev.* B **57** 64
[14] Ishizuka M, Yamada I, Amaya K and Endo S 1996 *J. Phys. Soc. Japan* **65** 1927
[15] Mitrofanov V Ya, Nikiforov A and Shashkin S Yu 1997 *Solid State Commun.* **104** 499
[16] Manaka H, Yamada I, Kitazawa T, Kobayashi M, Ishizuka M and Endo S 1997 *J. Phys. Soc. Japan* **66** 2989
[17] Valiente R and Rodríguez F 1996 *J. Phys. Chem. Solids* **57** 571
[18] Morón M C, Palacio F, Clark S M and Paduan-Filho A 1995 *Phys. Rev.* B **51** 8660
Morón M C, Palacio F, Clark S M and Paduan-Filho A 1996 *Phys. Rev.* B **54** 7052
[19] Rodríguez F, Hanfland M, Itié J P and Polian A 2001 Optical properties of A_2CuCl_4 layer perovskites under pressure. Structural correlations *Frontiers of High Pressure Research II. Application of High Pressure to Low-Dimensional Novel Electronic Materials* ed H D Hochheimer, B Kuchta, P K Dorthout and J L Yarger (Dordrecht: Kluwer–Academic) p 143
[20] Pinsard-Gaudart L, Rodríguez-Carvajal J, Daoud-Aladine A, Goncharenko I, Medarde M, Smith R I and Revcolevschi A 2001 *Phys. Rev.* B **64** 064426
[21] Loa I, Adler P, Grzechnik A, Syassen K, Schwarz U, Hanfland M, Rozenberg G Kh, Gorodetsky P and Pasternak M P 2001 *Phys. Rev. Lett.* **87** 125501
[22] Witteveen H T, Jongejan D L and Brandwijk V 1974 *Mater. Res. Bull.* **9** 345
[23] Waizumi K, Masuda H, Ohtaki H, Burkov K A and Chernykh L 1992 *Acta Crystallogr.* C **48** 1374
[24] Rodríguez-Carvajal J 1993 Full Prof *Physica* B **192** 55
[25] Pabst I, Fuess H and Bats W 1987 *Acta Crystallogr.* C **43** 413
[26] Steadman J P and Willett R D 1970 *Inorg. Chim. Acta* **4** 367
[27] Barendregt F and Schenk H 1970 *Physica* **49** 465